PERGAMON

International Journal of Heat and Mass Transfer 44 (2001) 4333–4343

International Journal of HEAT and MASS TRANSFER

www.elsevier.com/locate/ijhmt

Correlation between heat transfer and pressure drop in channels with periodically grooved parts

Takahiro Adachi [a,*], Haruo Uehara [b]

[a] *OTEC Laboratory, Saga University, Honjo, Saga 840-8502, Japan*
[b] *Department of Mechanical Engineering, Saga University, Honjo, Saga 840-8502, Japan*

Received 16 June 2000; received in revised form 5 January 2001

Abstract

Correlation between heat transfer and pressure drop in channels with periodically grooved parts along the streamwise direction is investigated for various channel configurations by assuming two-dimensional and periodically fully developed flow and temperature fields. Streamwise periodic variations of the cross-section induce the bifurcation from steady-state flow to oscillatory one. Heat transfer is enhanced significantly after the bifurcation with the increase of pressure drop. An efficiency defined as the ratio of the heat transfer enhancement to the increase of pressure drop is considered. It is found that the channels with expanded grooves perform efficiently, while the channels with contracted grooves inefficiently. © 2001 Elsevier Science Ltd. All rights reserved.

1. Introduction

Several techniques have been developed to augment single phase convective heat transfer in channels and to reduce the size and weight of heat exchangers. A commonly used technique for improving the performance of heat exchange devices is to set up periodic disturbance promoters along the streamwise direction. Such an arrangement of the channels might lead to the enhancement of the heat transfer due to flow mixing and periodic interruptions of thermal boundary layers, but often causes increase of pressure drop penalty [1].

The channels which have streamwise periodic cross-sections can be divided into identical modules in the streamwise direction where the fully developed flow and temperature fields repeat periodically after a certain entrance region. This assumption enables us to confine the calculation domain to cover only one of these modules without dealing with the entrance region. Such a procedure was first suggested by Patankar et al. [2] and was applied to a configuration consisting of successive ranks of isothermal plate segments placed transverse to the main flow direction under steady-state condition.

There are numerous investigations using the periodic and fully developed concepts on fluid flow and heat transfer for the parallel plate channels with periodically grooved parts. Ghadder et al. [3], Sunden and Trollheden [4] and Pereira and Sousa [5] investigated the flow in channels with rectangular grooves on one plate. They showed complex flow patterns such as separation, recirculation, re-attachment and deflection. Especially, Ghadder et al. found the presence of self-sustained oscillatory flow. In addition, Ghadder et al. [6] showed that the resonant oscillation of the self-sustained flow results in doubling the heat transfer. Moreover, Farhanieh [7] investigated numerically heat transfer and fluid flow for channels with trapezoidal grooved parts for laminar steady-state flow. Greiner et al. [8] and Wirtz et al. [9] reported the measured pressure drop and heat transfer performance of the channels having a series of V-grooves formed on both walls or only one wall.

In this work, the fluid flow and heat transfer in channels with contracted and expanded grooves set up both symmetrically and asymmetrically with the centerline of the parallel plates are investigated as a simple model of plate-type heat exchangers. The flow and temperature fields are assumed to be two-dimensional and periodically fully developed. The temperature on the channel walls is kept constant. Correlations between heat transfer and pressure drop are reported to reveal

* Corresponding author.

0017-9310/01/$ - see front matter
PII: S0017-9310(01)00070-9

Nomenclature

a_u	fupper height of contracted or expanded groove from the centerline
a_l	lower height of contracted or expanded groove from the centerline
D_h^*	hydraulic diameter $4h^*$
h	half height of the parallel plane channel
L	period of the module
l	length of contracted or expanded groove
Nu	local Nusselt number
Nu_m	mean Nusselt number
n	distance normal to the wall
Pe	Peclet number
Pr	Prandtl number
p	pressure
Re	Reynolds number
s	distance along the grooved channel wall from the inlet
T	nondimensional temperature
T_0	period of oscillation
T_b	local bulk temperature
T_i	temperature at inlet
T_w	wall temperature
U_m^*	mean velocity at the cross-section with height $2h^*$
U^*	representative velocity
u, v	velocity components in x- and y-directions, respectively
$\mathbf{u}$	velocity vector

Greek symbols

α^*	heat transfer coefficient
Δp	pressure drop
ϵ	relaxation factor
η	efficiency between the heat transfer and pressure drop
Θ	normalized temperature as $(T - T_w)/(T_b - T_w)$
κ^*	thermal diffusivity
λ^*	thermal conductivity
ν^*	kinematic viscosity
ρ^*	density
ψ	nondimensional stream function
ω	nondimensional vorticity

Subscripts

c	critical
p	parallel plate channel
*	dimensional value

numerically the efficient channel configurations with periodically grooved parts.

2. Governing equations

We consider a two-dimensional channel shown in Fig. 1. The channel consists of parallel plates of height $2h^*$ with periodically contracted or expanded grooves. Fig. 1(f) is one of the periodic modules with periodicity length L^*. Fluid enters from an inlet far upstream and flows through the entrance region, and arrives at the module.

The x-axis is taken in the flow direction along the centerline of the parallel plate channel and the y-axis is perpendicular to it with the origin O in Fig. 1(f). The flow is assumed to be two-dimensional and incompressible. We make the following physical quantities nondimensional by taking half height of the plates h^*, velocity $U^* = 3/2\,U_m^*$ (U_m^* is mean velocity at the cross-section with height $2h^*$), temperature on the plates T_w^* and one for the fluid at the inlet of the channel T_i^* as representative quantities, that is,

$$x = \frac{x^*}{h^*}, \quad y = \frac{y^*}{h^*}, \quad t = \frac{t^* U^*}{h^*}, \quad \omega = \frac{\omega^* h^*}{U^*}, \quad \psi = \frac{\psi^*}{U^* h^*}, \quad T = \frac{T^* - T_w^*}{T_i^* - T_w^*}, \tag{1}$$

where we represent physical quantities with their dimensions by attaching a superscript * to them. Then, the governing equations for vorticity $\omega(x, y, t)$, stream function $\psi(x, y, t)$ and temperature $T(x, y, t)$ are written in nondimensional form as

$$\frac{\partial \omega}{\partial t} + J(\omega, \psi) = \frac{1}{Re} \nabla^2 \omega, \tag{2}$$

$$\omega = -\nabla^2 \psi, \tag{3}$$

$$\frac{\partial T}{\partial t} + J(T, \psi) = \frac{1}{PrRe} \nabla^2 T, \tag{4}$$

where the operator $J(f, g) = \partial f/\partial x \partial g/\partial y - \partial g/\partial x \partial f/\partial y$. The Reynolds number and Prandtl number are defined as $Re = U^* h^*/\nu^*$ and $Pr = \nu^*/\kappa^*$, where ν^*, κ^* are the kinematic viscosity and thermal diffusivity of the fluid, respectively.

Moreover, as parameters to determine the configuration of the channel, period of the channel L, length of the contracted or expanded grooves l, and heights of the grooves from the centerline of the parallel plates a_u, a_l are defined as

$$L = L^*/h^*, \quad l = l^*/h^*, \quad a_u = a_u^*/h^*, \quad a_l = a_l^*/h^*, \tag{5}$$

where the channel consists of parallel plates for $a_u = a_l = 1$, whereas it has expanded grooves if $a_u, a_l > 1$ and contracted grooves if $a_u, a_l < 1$.

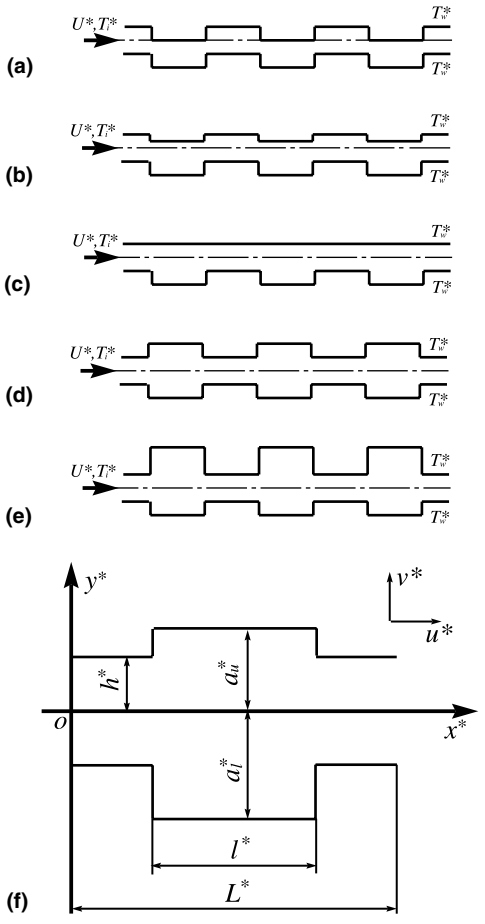

Fig. 1. Geometries and co-ordinates. (a) Asymmetric channel with expanded and contracted grooves in both plates ($a_u = 0$). (b) Asymmetric channel with expanded and contracted grooves in both plates ($a_u = 0.5$). (c) Asymmetric channel with expanded grooves in one plate ($a_u = 1$). (d) Symmetric channel with expanded grooves in both plates ($a_u = 2$). (e) Asymmetric channel with expanded grooves ($a_u = 3$). (f) One of the modules.

A pressure field is obtained by solving the Navier–Stokes equation as

$$\nabla p = -\frac{\partial \mathbf{u}}{\partial t} - (\mathbf{u}\cdot\nabla)\mathbf{u} + \frac{1}{Re}\nabla^2\mathbf{u}, \tag{6}$$

where the velocity $\mathbf{u} = (u, v)$ is expressed in terms of the stream function ψ as $u = \partial\psi/\partial y$ and $v = -\partial\psi/\partial x$.

We assume that the velocity is zero and the temperature is kept to be constant on the plates. We adopt in this study the case that flow rate is fixed in time, but pressure difference between the inlet and outlet of the channel fluctuates. Then, the imposed flow rate $2U_m^* h^*$ is constant and its nondimensional value is 4/3 in this case. The boundary conditions on the plates are written as

$$\psi = 0, \quad u = \frac{\partial\psi}{\partial y} = 0, \quad v = -\frac{\partial\psi}{\partial x} = 0, \quad T = 0$$

on the lower plate, (7)

$$\psi = \frac{4}{3}, \quad u = \frac{\partial\psi}{\partial y} = 0, \quad v = -\frac{\partial\psi}{\partial x} = 0, \quad T = 0$$

on the upper plate. (8)

The flow is expected to attain, after a short entrance region, a periodic fully developed regime, in which the velocity field repeats itself from module to module. This expectation is validated by the results of Greiner et al. [8] and Farhanieh et al. [12], where the flow became periodic after only three to five modules in the entrance region. So, the following periodic boundary conditions are imposed at the inlet and outlet of the module

$$\psi(x + L, y, t) = \psi(x, y, t), \tag{9}$$

$$\omega(x + L, y, t) = \omega(x, y, t). \tag{10}$$

The fluid temperature in the fully developed periodic flow with a constant wall temperature does not simply repeat itself but the normalized temperature profile which is defined by $(T - T_w)/(T_b - T_w)$ repeats identically from module to module. Then, the inlet and outlet boundaries have the following relations.

$$\frac{T(x + L, y, t) - T_w}{T_b(x + L) - T_w} = \frac{T(x, y, t) - T_w}{T_b(x) - T_w}, \tag{11}$$

where $T_b(x)$ is the cross-sectional local bulk temperature defined as

$$T_b(x) = \frac{\int |u| T \, dy}{\int |u| \, dy}. \tag{12}$$

The absolute value of the velocity u is used here so that the regions with reverse flow are properly represented. The integrals are to be carried over the cross-sectional area of the channel. Kelkar and Patankar [10] and Wang and Tao [11] described the computational details about the periodic boundary conditions.

A reference value for the pressure p is taken as $p = 0$ at the centerline of the inlet of the module.

3. Numerical methods

We solve the governing equations numerically by the time marching method for an appropriate initial condition as $\omega = \psi = 0, T = 0.5$. The vorticity transport Eq. (2) and the energy Eq. (4) are approximated by the explicit Adams–Bashforth method with the second-order accuracy in time together with the second-order accuracy of central finite difference in space, but the convective term in Eq. (4) is approximated by the

first-order upwind method. The Poisson equation (3) is approximated by the second-order central difference and solved by the successive over relaxation (SOR) method, where the relaxation factor ϵ is constant and $\epsilon = 1.5$ is used. The convergence of the SOR method is determined when the maximum relative difference for the stream function reaches 10^{-5}.

The steady state is determined when the velocity v and the normalized temperature $\Theta = (T - T_w)/(T_b - T_w)$ at $(x, y) = (L/2 + l/2, -0.5)$ become independent of time and the maximum relative difference of two successive time steps reaches 10^{-8}. In the case that the flow and temperature fields are in time periodic oscillatory state, it is judged as fully time periodic when the maximum relative difference for local maximum amplitudes of v and Θ between two oscillation cycles reaches 10^{-4}.

In all the calculations, equally spaced mesh system with $\Delta x = \Delta y = 0.05$ and the time increment $\Delta t = 0.0001$ are used. The grid fineness in space is checked by calculating with different values of Δx and Δy for $L = 8, l = 4, a_u = 1, a_l = 2$, $Re = 400$ and $Pr = 7$. The numerical solution of the trial calculation gives $v = 0.0123$ and $\Theta = 0.935$ with $\Delta x = \Delta y = 0.05$ and $v = 0.0121$ and $\Theta = 0.933$ with $\Delta x = \Delta y = 0.04$. It shows that relative error for v and Θ is within only 2% with the difference of grid sizes. The higher-order results may be estimated by Richardson extrapolation method according to these numerical values as $v_{est} = 0.0117$ and $\Theta_{est} = 0.928$, where the accuracy is taken as 2 for v and 1.5 for Θ because the convective term for energy equation is discretized by the first order upwind difference. Then the estimated error may be as large as 8%.

In addition, we compare our numerical results with other numerical and analytical ones. We obtain the frequency of v as 0.1415 for $L = 6.6, l = 2.2, a_u = 1$, $a_l = 2.1$ and $Re = 525$ from a reciprocal of oscillation period which is given by a typical crest-to-crest distance. It shows good agreement with 0.142 of Ghadder et al. [3] for $L = 6.6666, l = 2.2222, a_u = 1, a_l = 2.1111$ and $Re = 525$ which was obtained by using the spectral element method. Furthermore, the mean Nusselt number which is defined in Section 4.2 is 7.52 for parallel plate channel ($a_u = a_l = 1, L = 8$) at $Re = 400$ and $Pr = 7$, which shows within 0.3% relative error with the analytical value of 7.54 [13]. From the above numerical check, it is confirmed that our numerical results are valid.

4. Results

4.1. Flow and temperature fields

Numerical simulations are carried out for the channel configurations $L = 8$, $l = 4$, $a_l = 2$ which are fixed, and for five different values of $a_u = 0, 0.5, 1, 2$ and 3. The

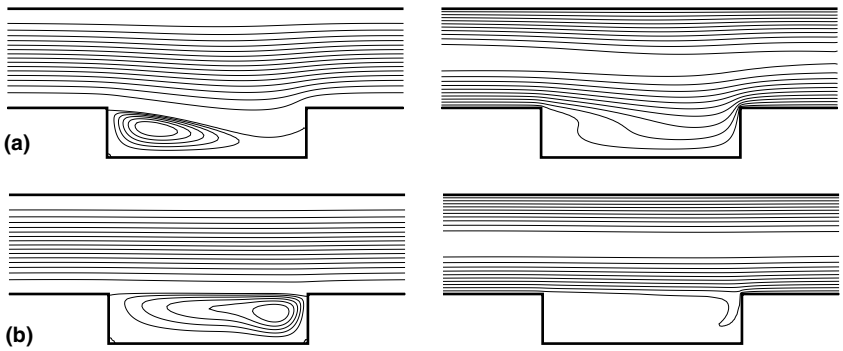

Fig. 2. Flow and temperature fields for $a_u = 1$. Streamlines are on the left side and isotherms are on the right side. (a) $Re = 50$. (b) $Re = 380$.

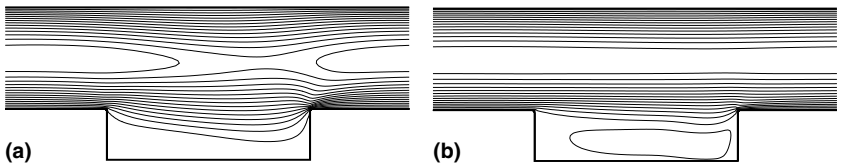

Fig. 3. Velocity fields for $a_u = 1$. (a) $Re = 50$. (b) $Re = 380$.

Reynolds number is up to 500 and the Prandtl number is 7.

4.1.1. Steady state

The streamlines ($\psi = \text{const.}$) and isotherms ($T = \text{const.}$) of the steady-state flow and temperature fields for $a_u = 1$ at $Re = 50$ and 380 are depicted in Fig. 2. The flow is from left to right. Hereafter, the contour levels for flow field have been chosen to detail the recirculating region, but those for temperature field are equal difference. The streamlines are shown on the left side and the isotherms on the right side. In this case, the upper plate is parallel and the lower one has the expanded groove, so the channel is asymmetric.

A vortical flow motion can be seen at the upstream side of the expanded groove for $Re = 50$ and the main flow deflects into groove. The vortex grows larger and its center moves to the downstream as the Reynolds number increases and occupies whole region of the groove for $Re = 380$. The main flow at $Re = 380$ is straight without deflecting and becomes parallel such as the profile of a plane Poiseuille flow. Fig. 3 shows the velocity profiles ($U = \text{const.}$) for $Re = 50$ and 380, where the contour levels are equal difference. They also suggest that the flow is close to core Poiseuille flow, with the grooved region occupied with slow moving fluid, as the Reynolds number increases. There are some previous studies for this configuration as $a_u = 1$, and qualitative behavior such as the vortical flow motion and the formation of the slow moving fluid region are the same as them [3–5].

The corresponding isotherms for $Re = 50$ deflect into the expanded groove. It is seen that diffusion is effective in heat transportation into the groove, thus showing that heat transportation extends throughout the whole area of the groove when fluid flows along the groove. On the other hand, as the Reynolds number increases, the isotherms do not get deflected into the groove because convection rather than diffusion becomes effective as shown in Fig. 2(b) for $Re = 380$, and heat transportation

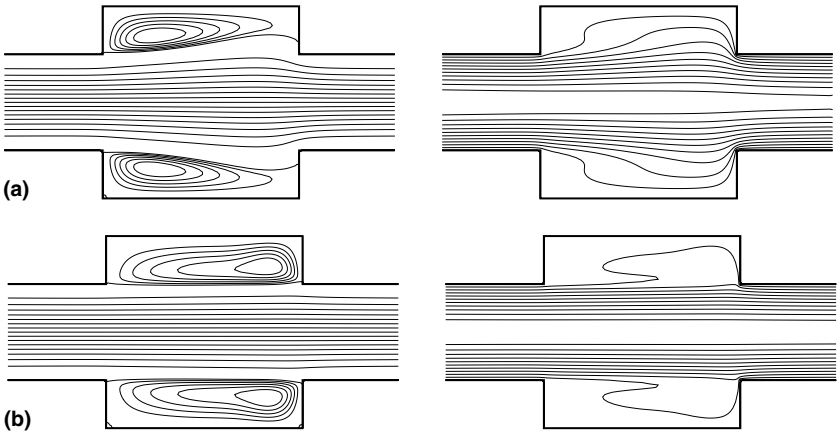

Fig. 4. Flow and temperature fields for $a_u = 2$. Streamlines are on the left side and isotherms are on the right side. (a) $Re = 50$. (b) $Re = 260$.

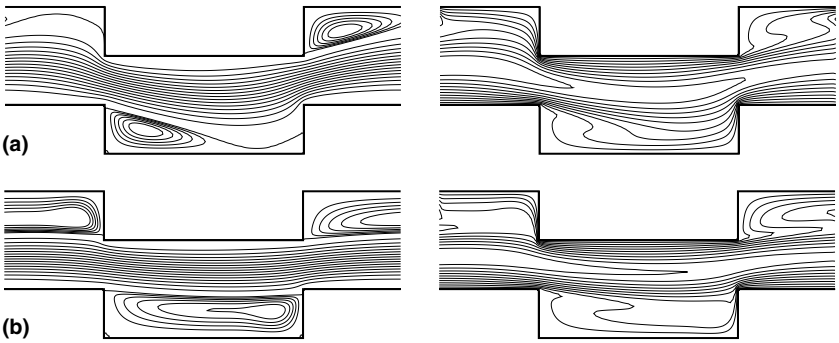

Fig. 5. Flow and temperature fields for $a_u = 0$. Streamlines are on the left side and isotherms are on the right side. (a) $Re = 50$. (b) $Re = 100$.

does not extend into the upstream side of the groove. It is observed that the thermal boundary layer which develops along the channel is interrupted and re-established due to the existence of the groove.

The streamlines of the steady flow for $a_u = 2$ at $Re = 50$ and 260 are shown on the left side in Fig. 4. In this case, the channel has expanded grooves in both the upper and lower plates, and it is symmetric with the centerline. For the two Reynolds numbers studied, the flow is symmetric with the centerline of the channel without deflecting into one side, although it is pointed out to become asymmetric depending on the channel configurations by a pitchfork bifurcation [14]. The corresponding isotherms are presented on the right side in Fig. 4. Our pictures shown here are similar to the results in periodic wavy passages [15].

The streamlines of the steady flow for $a_u = 0$ at $Re = 50$ and 100 are depicted on the left side in Fig. 5. In this case, the upper plate has a contracted groove and the lower has an expanded one, so the channel is asymmetric. It is seen that the streamlines meander along the channel configuration in Fig. 5(a) and the main flow goes deeply in the grooves. The corresponding isotherms are presented on the right side in Fig. 5. It is seen that isotherms strikingly converge on the region with the most narrow height h^* compared with the other cases because the upper plate is contracted and the main flow is restricted almost the half region with height h^*.

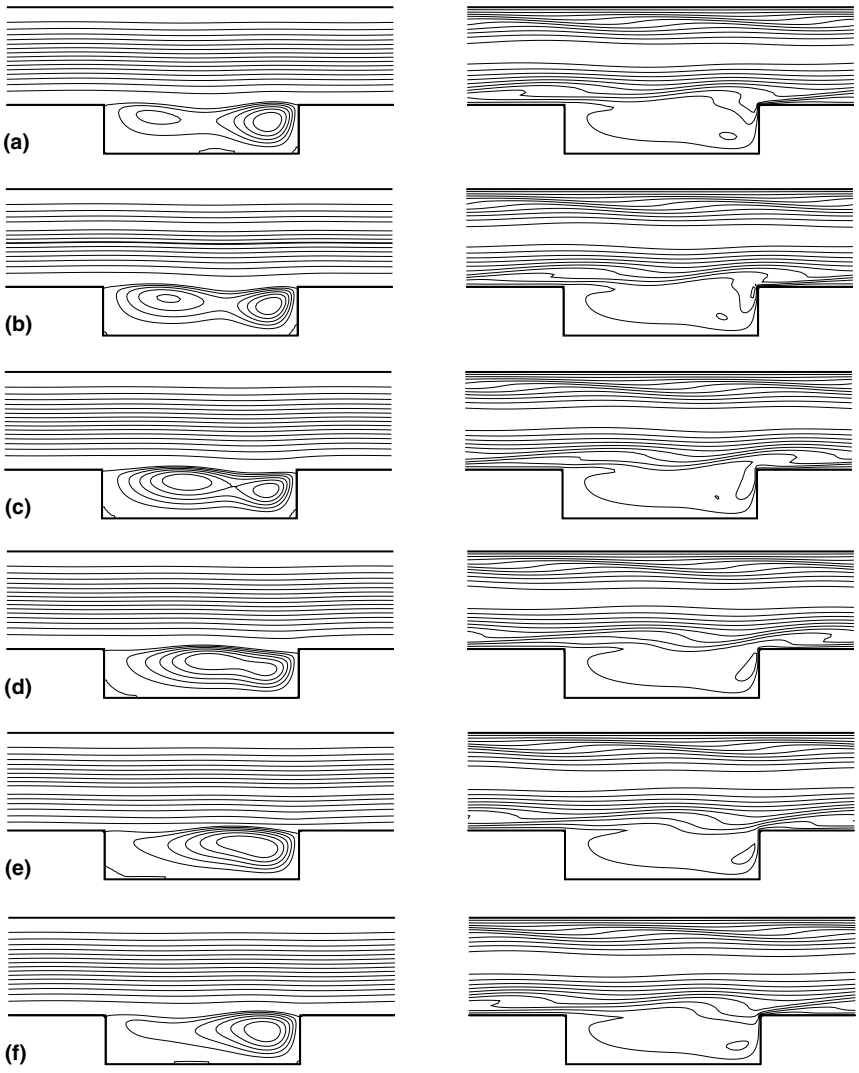

Fig. 6. Flow and temperature fields during one oscillation cycle for $a_u = 1$ at $Re = 420$ ($Re_c = 409$). Streamlines are on the left side and isotherms are on the right side. (a) $t = t_0 + 0/6T_0$. (b) $t = t_0 + 1/6T_0$. (c) $t = t_0 + 2/6T_0$. (d) $t = t_0 + 3/6T_0$. (e) $t = t_0 + 4/6T_0$. (f) $t = t_0 + 5/6T_0$.

4.1.2. Oscillatory state

Adachi and Uehara [16] studied the instability and transition of the steady-state flow together with the pressure drop characteristics in the same channel configurations as we consider in this paper, and showed that the steady-state flow becomes unstable for Tollmien–Schlichting wave modes and bifurcates to a time-periodic, self-sustained oscillatory flow at a critical Reynolds number Re_c due to Hopf bifurcation. They obtained the following relations with the critical Reynolds numbers to the various geometric parameters a_u.

$$Re_c = 187a_u^{-1.43} + 222 \quad \text{for } 1 \leqslant a_u \leqslant 3. \tag{13}$$

$$Re_c = 123(a_u + 1)^{1.74} \quad \text{for } 0 \leqslant a_u \leqslant 1. \tag{14}$$

Here we show instantaneous streamlines and isotherms of the self-sustained oscillatory flow with period T_0 at every one-sixth period arbitrarily from time t_0 for $a_u = 0, 1$ and 2 in Figs. 6–8, where the Reynolds numbers are slightly larger than the critical values. The streamlines are depicted on the left side and the isotherms are on the right side. For $a_u = 0$ and 2, the same phenomena repeat for every half period inside the upper and lower grooves alternately, so we show only the results for the half period and omit those for the other half period.

The vortices in the grooves repeat the process that they move to the downstream so as to press the wall of grooves, and simultaneously new vortices are born in the upstream half of the groove as shown on the left side in Figs. 6–8. For the corresponding isotherms on the right side of the figures, there are significant waviness and roll-up of the isotherms at the groove lip, so the isotherms deflect deeply into the grooves, which are typically observed for the case of $a_u = 2$. Moreover, it is observed that the thermal boundary layers are re-established more intensively than the case for the steady state. Especially, the isotherms are very thin at the outer corner where the re-establishment of thermal boundary layer starts because the secondary vortices inside the grooves are pressed to the corner. Thus, it can be seen that the self-sustained oscillatory motions of the secondary vortices inside the grooves remarkably contribute to the enhancement of heat transfer and flow mixing.

4.2. Heat transfer and pressure drop

We consider the effect of contracted or expanded grooves on the pressure. The pressure drop Δp is defined as

$$\Delta p = \frac{(p_i^* - p_o^*)}{\rho^* U^{*2}} = p_i - p_o, \tag{15}$$

where p_i and p_o are the cross-sectional averaged nondimensional pressure at the inlet and outlet of the periodic

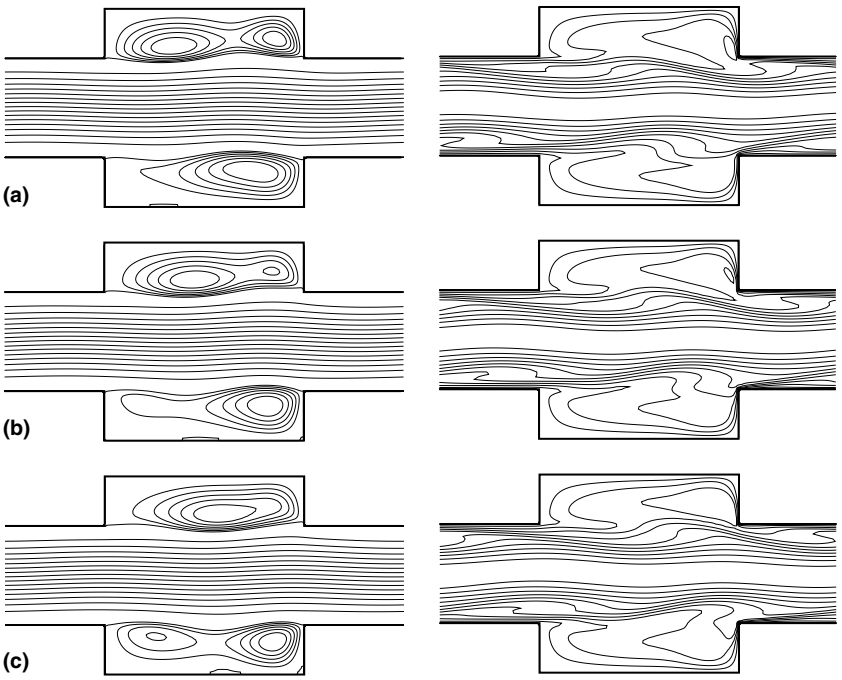

Fig. 7. Flow and temperature fields during half oscillation cycle for $a_u = 2$ at $Re = 300$ ($Re_c = 289$). Streamlines are on the left side and isotherms are on the right side. (a) $t = t_0 + 0/6T_0$. (b) $t = t_0 + 1/6T_0$. (c) $t = t_0 + 2/6T_0$.

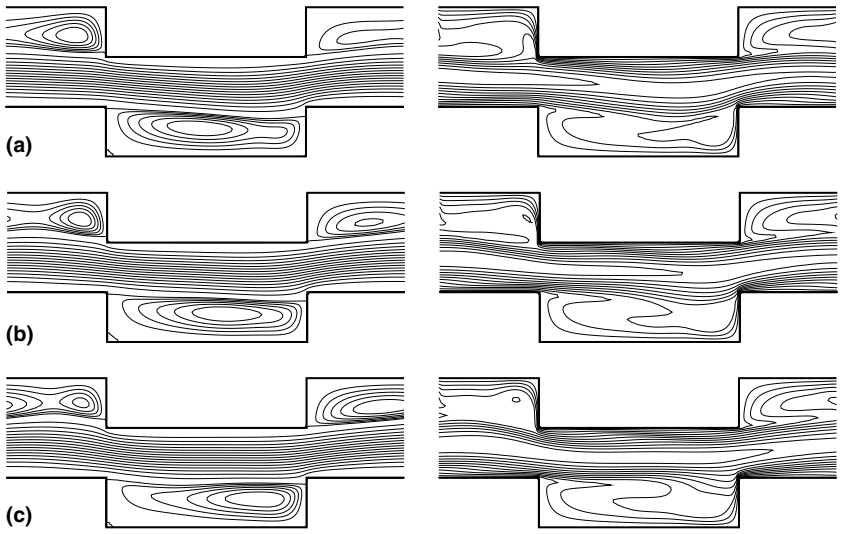

Fig. 8. Flow and temperature fields during half oscillation cycle for $a_u = 0$ at $Re = 130$ ($Re_c = 123$). Streamlines are on the left side and isotherms are on the right side. (a) $t = t_0 + 0/6T_0$. (b) $t = t_0 + 1/6T_0$. (c) $t = t_0 + 2/6T_0$.

module, respectively. The time-averaged value is used when the flow field is time periodic.

For practical applications, it is desirable to compare the pressure drops with corresponding values Δp_p for the parallel plate channel whose height is $2h^*$ throughout in this study. The ratios $\Delta p/\Delta p_p$ of the pressure drops are provided against the Reynolds numbers in Fig. 9, where $\Delta p_p = 2L/Re$ exactly derived from the Navier–Stokes equation. The pressure drop ratios for $a_u = 1, 2$ and 3 are less than unity for $Re < Re_c$, while they increase above unity for $Re > Re_c$. It is consistent with the previous results of Ghadder et al. for the configuration as $a_u = 1$ [3]. On the other hand, the pressure drop ratios for $a_u = 0$ and 0.5 which have contracted grooves, are always larger than unity. Our paper [16] gives more information on the pressure drop.

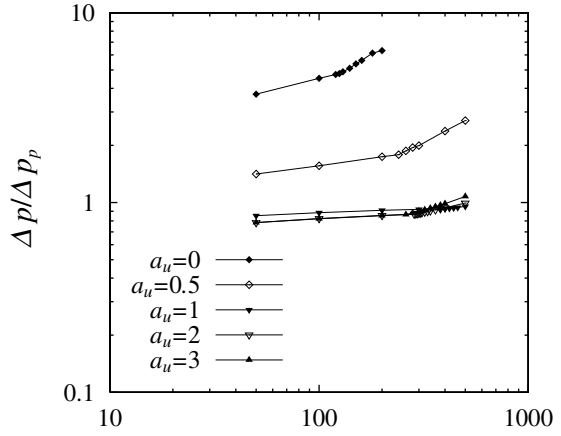

Fig. 9. The pressure drop ratios.

Next we consider the effect of grooves on the heat transfer. A local Nusselt number, Nu is defined as

$$Nu = \frac{\alpha^* D_h^*}{\lambda^*}, \tag{16}$$

where α^* is the heat transfer coefficient, λ^* the thermal conductivity of the fluid and $D_h^* = 4h^*$, the hydraulic diameter. A local heat flux q^* is defined as

$$q^* = -\lambda^* \left(\frac{\partial T^*}{\partial n^*} \right)_{w,s} = \alpha^* (T_w^* - T_b^*), \tag{17}$$

where $(\partial T^*/\partial n^*)_{w,s}$ is the temperature gradient normal to the wall at the position s along the channel wall from the inlet of the module including the lateral wall. By introducing Eq. (17) in Eq. (16), we obtain

$$Nu = \frac{D_h^*}{T_w^* - T_b^*} \left(\frac{\partial T^*}{\partial n^*} \right)_{w,s} = \frac{4}{T_w - T_b} \left(\frac{\partial T}{\partial n} \right)_{w,s}. \tag{18}$$

The time averaged value is used when the temperature field is time periodic.

It is also desirable to compare the mean Nusselt numbers Nu_m integrated along the groove faces with corresponding values for the parallel plate channel $Nu_p = 7.54$ [13]. The ratios Nu_m/Nu_p of the mean Nusselt numbers for both the upper and lower plates are provided against the Reynolds numbers in Fig. 10.

The ratios for $a_u = 0.5, 1, 2$ and 3 are less than unity for $Re < Re_c$, thus the heat transfer is reduced in

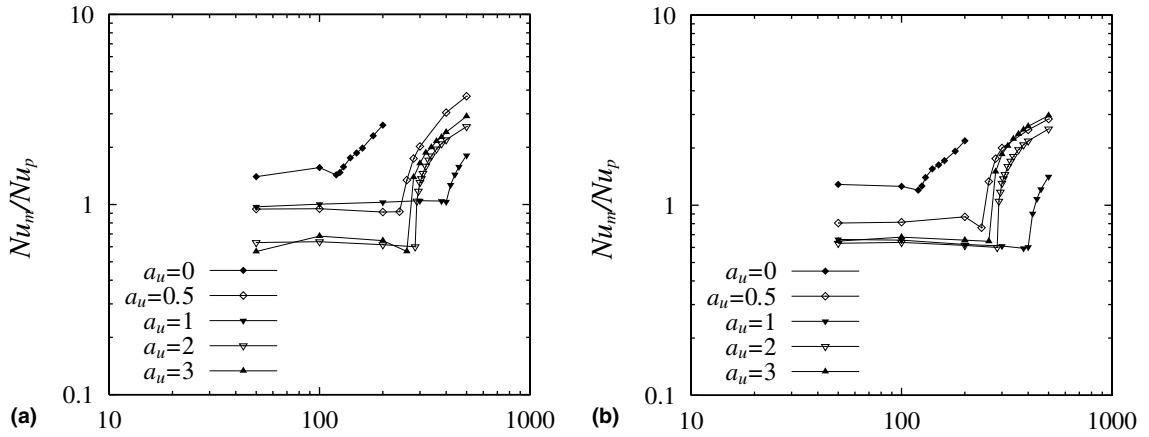

Fig. 10. The Nusselt number ratios. (a) For the upper plate. (b) For the lower plate.

comparison with the parallel plate channel, where the ratio for $a_u = 1$ in Fig. 10(a) is almost unity for $Re < Re_c$, because the upper plate for $a_u = 1$ is the same as the parallel plate. It is observed that the ratios decrease in some cases just before the critical Reynolds numbers. This is mainly because the effect of convection becomes intensive as the Reynolds number increases, and the local Nusselt numbers decrease inside the grooves. However, once the flow fields become oscillatory state for $Re > Re_c$, the ratios increase abruptly to overcome unity for $a_u = 0.5, 1, 2$ and 3. On the other hand, the ratio for $a_u = 0$ is always greater than unity in spite of the flow state. We can conclude that the heat transfer for periodically grooved channel is enhanced highest possibly four times larger than those for the parallel plate channel as the Reynolds number is beyond its critical value, and other experimental and numerical studies confirm these levels of augmentation [7,9].

It has been found that the heat transfer is enhanced when the self-sustained oscillatory flow occurs. In order to study why the mean Nusselt numbers increase for the oscillatory flow, the local Nusselt number ratios Nu/Nu_p evaluated along one side of the plates are presented for $a_u = 2$ at $Re = 50$, 260 and 300 in Fig. 11, where the channel is symmetric with the centerline in this case, and s is the distance from the inlet to outlet along the channel wall including the lateral one. The flow and temperature fields are in steady state for $Re = 50$ and 260, and in oscillatory state for $Re = 300$.

The local Nusselt number ratios for $Re = 50$ and 260 approach $Nu/Nu_p \sim 1$ except the expanded groove. They decrease sharply inside the groove ($2 < s < 8$), so the mean values of Nu/Nu_p are less than unity in spite of the local maximum shown at the upstream and downstream outer corners (vicinity of $s = 2, 8$). On the other hand, Nu/Nu_p for $Re = 300$ shows very strikingly

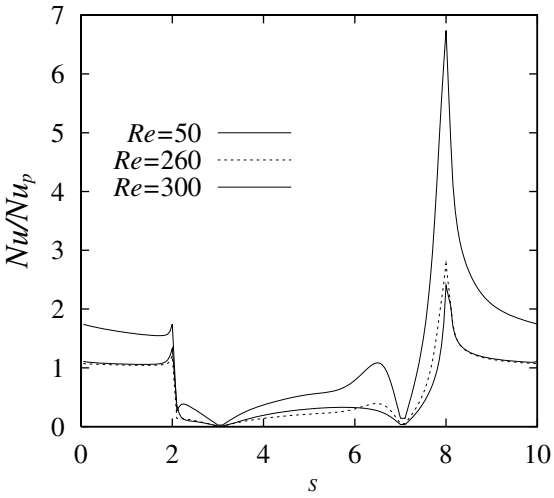

Fig. 11. The local Nusselt number distributions for $a_u = 2$.

large value at the downstream outer corner (vicinity of $s = 8$) compared with the other two cases and the local instantaneous Nusselt number always take larger value to the other two steady cases, mainly because the vortices inside the groove are promoted to the downstream so as to collect the isotherms. The larger value is followed by a gradual decrease except the groove toward the next one, so that the mean values of Nu/Nu_p become greater than unity although Nu/Nu_p decreases inside the groove temporarily. The mechanism of heat transfer enhancement is summarized as follows. When once the steady flow bifurcates to the oscillatory one, the vortex inside the groove begins to move downstream due to traveling Tollmien–Schlichting wave generated in the main flow. Namely, a translational velocity toward the downstream direction

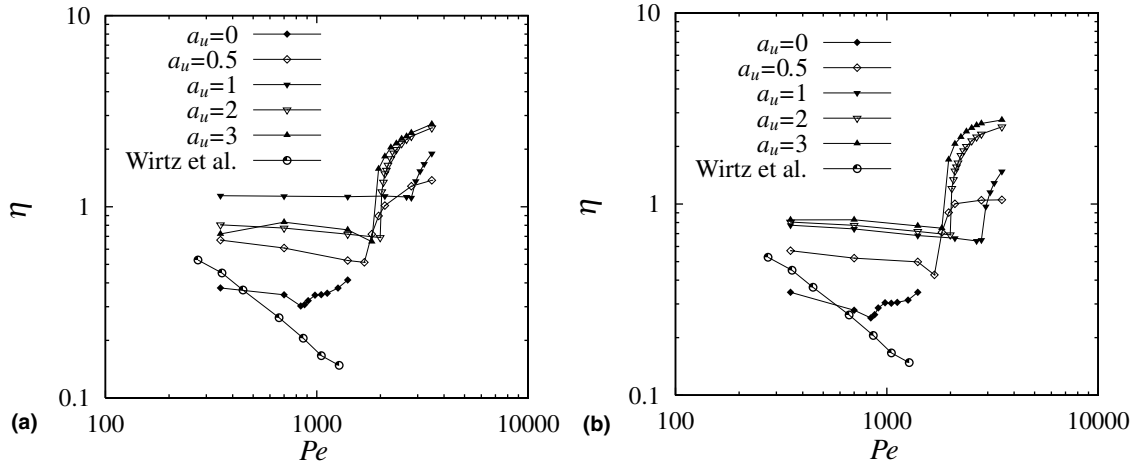

Fig. 12. The efficiency between heat transfer and pressure drop. (a) For the upper plate. (b) For the lower plate.

is generated in the grooved part. Therefore, the isotherms are translated by the velocity into the downstream outer corner, so that the thermal boundary layer becomes more thin leading to the larger heat flux than the steady-state cases.

It is practically important to reveal the channel configurations which show the efficient performance between the heat transfer and pressure drop. We define an efficiency η as the ratio of the heat transfer enhancement to the increase of pressure drop as

$$\eta = \frac{Nu_{\mathrm{m}}/Nu_{\mathrm{p}}}{\Delta p/\Delta p_{\mathrm{p}}}. \tag{19}$$

We show the efficiency η against the Peclet number $Pe = RePr$ in Fig. 12 for both the upper and lower plates, to compare with the results of Wirtz et al. [9]. They obtained experimentally the Colburn j-factors from the mean Nusselt numbers based on the centerline temperature for air flows for the channel having a series of transverse V-grooves. In their study, expanded grooves are symmetrically placed on both the channel walls and each groove is right angled triangle with depth $2.4h^*$. They tabulated the friction factor and Colburn j-factors. Here we recalculate the mean Nusselt numbers for $Pr = 0.7$ and show η against Pe in Fig. 12.

In these figures, the region for $\eta > 1$ means that the heat transfer enhancement exceeds the increase of pressure drop, and the efficiency is superior to the parallel plate channel. For the channels with contracted grooves for $a_{\mathrm{u}} < 1$, the heat transfer is enhanced compared with the other configurations for both the upper and lower plates, but the pressure drop is also larger than the others. So, η is less than unity for almost extent of Pe considered here. For $a_{\mathrm{u}} = 1$, η is always over unity for the upper plate, while it is less than unity for the lower plate until the onset of self-sustained oscillations. Once the flow becomes oscillatory state, η for $a_{\mathrm{u}} = 1$ becomes over unity. For $a_{\mathrm{u}} = 2$ and 3, η is less than unity for the steady-state flow, while increases over unity for the oscillatory one. It is found that the regions for $\eta > 1$ are realized for relatively small Pe in these cases.

In the case of Wirtz et al. [9], the critical Reynolds number for the onset of the oscillatory flow is $Re_{\mathrm{c}} = 177$ and η for the oscillatory to turbulent flow regimes is shown in Fig. 12. So, the heat transfer is thought to be enhanced compared with the parallel plate channel because the flow becomes better mixed, but the pressure drop increases over the heat transfer enhancement. This is mainly expected to be due to the effect of the groove shape instead of that of the Prandtl number, because the

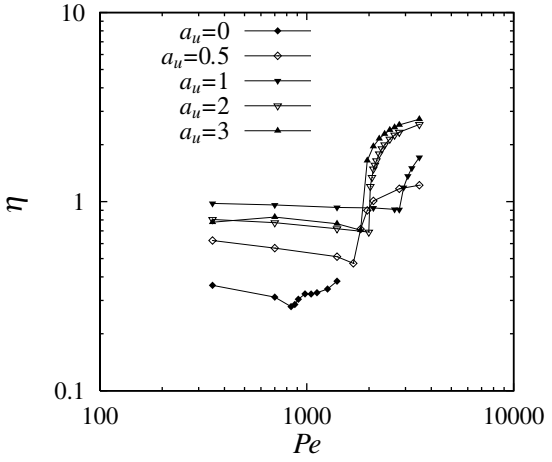

Fig. 13. The overall efficiency combining both upper and lower plates.

pressure drop characteristics are independent of the Prandtl number.

Finally, we show the over all efficiency combining both upper and lower plates in Fig. 13 in order to show the efficient channel configuration. It is found that the channels for $a_u = 2$ and 3 show efficient performance over the parallel plane channel especially in the oscillatory flow state.

5. Conclusions

A numerical investigation has been performed for the flow and temperature fields in channels with periodically grooved parts along the streamwise direction as a simple model of plate-type heat exchangers. Numerical simulations of two-dimensional flow and temperature fields have been performed using finite difference method for the channel configurations $L = 8$, $l = 4$, $a_l = 2$ which are fixed, and for five different values of $a_u = 0, 0.5, 1, 2$ and 3. The Reynolds number range is $50 < Re < 500$ and the Prandtl number is being $Pr = 7$.

Numerical results have revealed that diffusion is effective in temperature field at relatively small Reynolds numbers, while convection is effective as the Reynolds numbers increase. Thus the local Nusselt numbers inside the grooved parts are reduced in some cases as the Reynolds number increases. Once, however, the flow and temperature fields become oscillatory state, the mean Nusselt numbers increase abruptly. It is mainly because the vortices inside the grooves are promoted to the downstream wall so as to collect the isotherms and the re-establishment of the thermal boundary layer becomes intensive. The heat transfer is enhanced significantly after the bifurcation from steady-state flow to oscillatory one, but the pressure drop also increases. We have discussed the efficiency between the heat transfer enhancement and the increase of pressure drop for various channel configurations. It has been found that the channels with the expanded grooves show efficient performance over the parallel plane channel especially for the oscillatory flow state, while those with contracted grooves are inefficient.

Acknowledgements

The authors are thankful to Prof. Y. Ikegami and Ms. N. Visakha for their advice and support, and also to Ms. A. Ide, secretary in OTEC lab., for her words of encouragement.

References

[1] S., Kakac, R.K. Shah, W. Aung, Handbook of Single-Phase Convective Heat Transfer, Wiley-Interscience, New York, 1987 (Chapter 17).
[2] S.V. Patankar, C.H. Liu, E.M. Sparrow, Fully developed flow and heat transfer in ducts having streamwise-periodic variations of cross-sectional area, ASME J. Heat Transfer 99 (1977) 180–186.
[3] N.K. Ghaddar, K.Z. Korczak, B.B. Mikic, A.Y. Patera, Numerical investigation of incompressible flow in grooved channels. Part 1. Stability and self-sustained oscillations, J. Fluid Mech. 163 (1986) 99–127.
[4] B. Sunden, S. Trollheden, Periodic laminar flow and heat transfer in a corrugated two-dimensional channel, Int. Comm. Heat Mass Transfer 16 (1989) 215–225.
[5] J.C.F. Pereira, J.M.M. Sousa, Finite volume calculations of self-sustained oscillations in a grooved channel, J. Comput. Phys. 106 (1993) 19–29.
[6] N.K. Ghaddar, M. Magen, B.B. Mikic, A.Y. Patera, Numerical investigation of incompressible flow in grooved channels. Part 2. Resonance and oscillatory heat-transfer enhancement, J. Fluid Mech. 168 (1986) 541–567.
[7] B. Farhanieh, B. Sunden, Numerical investigation of periodic laminar heat transfer and fluid characteristics in parallel plate ducts with streamwise-periodic cavities, Int. J. Numer. Meth. Heat Fluid Flow 1 (1991) 143–157.
[8] M. Greiner, R.F. Chen, R.A. Wirtz, Enhanced heat transfer/pressure drop measured from a flat surface in a grooved channel, ASME J. Heat Transfer 113 (1991) 498–501.
[9] R.A. Wirtz, F. Huang, M. Greiner, Correlation of fully developed heat transfer and pressure drop in a symmetrically grooved channel, ASME J. Heat Transfer 121 (1999) 236–239.
[10] K.M. Kelkar, S.V. Patankar, Numerical prediction of flow and heat transfer in a parallel plate channel with staggered fins, ASME J. Heat Transfer 109 (1987) 25–30.
[11] L.B. Wang, W.Q. Tao, Heat transfer and fluid flow characteristics of plate-array aligned at angles to the flow direction, Int. J. Heat Mass Transfer 38 (1995) 3053–3063.
[12] B. Farhanieh, C. Herman, B. Sunden, Numerical and experimental analysis of laminar fluid flow and forced convection heat transfer in a grooved duct, Int. J. Heat Mass Transfer 36 (1993) 1609–1617.
[13] R.K. Shah, A.L. London, Laminar flow forced convection in ducts, Adv. Heat Transfer (Suppl. I) (1978) 153–195.
[14] J. Mizushima, H. Yamaguchi, H. Okamoto, Stability of flow in a channel with a suddenly expanded part, Phys. Fluids 8 (1996) 2933–2942.
[15] G. Wang, S.P. Vanka, Convective heat transfer in periodic wavy passages, Int. J. Heat Mass Transfer 38 (1995) 3219–3230.
[16] T. Adachi, H. Uehara, Transitions and pressure characteristics of flow in channels with periodically grooved parts, JSME Int. J. Series B (submitted for publication).